

# Visual Topography of V1 in the *Cebus* Monkey

RICARDO GATTASS, AGLAI P.B. SOUSA AND MARCELLO G.P. ROSA  
Instituto de Biofísica Carlos Chagas Filho, Universidade Federal do Rio de Janeiro,  
Rio de Janeiro, RJ 21.941 Brasil

## ABSTRACT

The representation of the visual field in the striate cortex (V1) was mapped with multiunit electrodes in the *Cebus* monkey. Nine *Cebus apella*, anesthetized with N<sub>2</sub>O and immobilized with pancuromium bromide were studied in repeated recording sessions.

In each hemisphere, V1 contains a continuous representation of the contralateral visual hemifield. The representation of the vertical meridian (VM) forms the external border of V1 except at the anteriormost portion of the calcarine fissure. The representation of the horizontal meridian (HM) divides the area so that the representation of the lower visual field is located dorsally, and that of the upper field ventrally.

The convoluted surface of V1 can be only partially unfolded, and no precise "flattened" map can be obtained without introducing surface discontinuities. The visual topography of V1 is presented in a series of coronal sections and in "flattened" maps.

The representation of the central visual field is magnified relative to that of the periphery in V1. The evaluation of the cortical magnification factors measured along isoecentric and isopolar dimensions in the partially unfolded model of V1 revealed anisotropies in the representation of the visual field with larger magnification along isopolar lines than along isoecentric lines. Receptive field size increases with increasing eccentricity, whereas point image size decreases with increasing eccentricity.

**Key words:** striate cortex, visuotopic organization, cortical magnification factor, point image size, receptive field size

Talbot and Marshall ('41) demonstrated that foveal and parafoveal regions of the contralateral visual hemifield are represented onto the lateral surface of the occipital lobe of the macaque. Daniel and Whitteridge ('61) extended the study of the visuotopic organization of V1 of Old World monkeys to the peripheral visual field representation, which they showed to be located along the calcarine sulcus. They showed that the visuotopic map of V1 is distorted, in the sense that it emphasizes the representation of central vision.

Among New World monkeys, the existence of a precise visuotopic projection in striate cortex was demonstrated by Cowey ('64) for the squirrel monkey, *Saimiri sciureus*. Later, Allman and Kaas ('71) described a complete visuotopic map of V1 for the owl monkey, *Aotus trivirgatus*, the only living nocturnal Simiiform primate. The emphasis in central vision representation in this species is smaller than that observed in either *Macaca* or *Cercopithecus* (Guld and Bertulis, '76; Dow et al., '81), a fact probably related to the

nocturnal habits of *Aotus*. However, a comparison between results obtained in New World and Old World monkeys must take into account the difference of visual habits, sulcal patterns (Falk, '80), and sizes of the cortical surface, when comparing the visual system of primates.

*Cebus apella* is a medium-sized New World monkey. In size, sulcal pattern, and habits, the *Cebus* is more comparable to either *Macaca* or *Cercopithecus* than to *Aotus*, a species with whom the *Cebus* shares a more recent common ancestor. Therefore, these species are adequate for a com-

Accepted October 1, 1986.

Address reprint requests to Dr. R. Gattass, Instituto de Biofísica Carlos Chagas Filho, Bloco G - CCS, Ilha do Fundão, Rio de Janeiro, RJ 21.941 Brasil.

In this work, the classification of primates suggested by Hoffstetter ('74) has been adopted.

parative study aiming to answer the following questions: Which of the reported differences in the cortical organization of the visual areas of *Aotus* and Old World monkeys are due to the acquisition of nocturnal habits by the first? and which are due to a fundamental difference between ceboid and cercopithecoid monkeys?

We have begun our comparative inquiry by studying the visuotopic organization of V1 in the *Cebus*. Our results indicate that the striate cortex of this species does not differ from that of Old World monkeys in size, location, and visuotopic organization. These observations suggest the existence, in a common ancestor present at the Upper Eocene, of potentialities to generate such an organization, which have been modified in *Aotus* due to its nocturnal habits.

Preliminary results have been previously described (Gattass et al., '84).

## MATERIALS AND METHODS

Nine *Cebus apella* monkeys weighing between 2.5 and 4 Kg were used. The first four animals were systematically studied with vertical electrode penetrations, which were distributed over a large portion of the striate cortex, both in the exposed cortical surface (the operculum) and in the calcarine sulcus. The following two animals were studied specifically in the region of representation of the peripheral-most portion of the visual field, and in the remaining three the recordings were restricted to the lateral surface, which represents eccentricities up to 5°. The topography of the visual field representation was determined by relating the positions of receptive fields of small clusters of neurons to the locations of the corresponding recording sites in the cortex.

The preanesthetic medication, induction and maintenance of anesthesia, immobilization, and electrode characteristics have all been described in detail previously (Gattass and Gross, '81). Briefly, prior to the first recording session a recording well and a bolt for holding the head were implanted under anesthesia and aseptic conditions. During the recording sessions, the animals were maintained under 70% nitrous oxide and 30% oxygen and immobilized with pancromium bromide. Varnish-coated tungsten microelectrodes with impedances of approximately .5 megohms at 500 Hz were used. Typically, 15–40 vertical penetrations were made through the intact dura mater, in 2–6 experimental sessions carried out over a 4-week period. The penetrations were spaced by approximately 1.5 mm, forming a grid extending throughout striate cortex and adjacent areas. In each penetration, recording sites were separated by 400 to 500  $\mu\text{m}$ .

### Visual stimuli

The details of the care with the eyes and of the visual stimuli have been previously described (Gattass and Gross, '81). Briefly, white and colored opaque stimuli were presented on a translucent hemisphere located 57 cm from the contralateral eye. The eye was focused at 57 cm by means of an appropriate contact lens. Visual stimuli could be presented up to about 100° along the horizontal meridian and up to elevations of 55° in the upper quadrant and down to 60° in the lower quadrant.

### Histology

The histological procedures were described in detail previously (Gattass and Gross, '81). Electrolytic lesions were

### Abbreviations

Ca	calcarine sulcus
CMF	cortical magnification factor
HM	horizontal meridian
IO	inferior occipital sulcus
IP	intraparietal sulcus
La	lateral sulcus
Lu	lunate sulcus
OT	occipito-temporal sulcus
Pa	paraoccipital sulcus
PO	parieto-occipital sulcus
PRO	area prostriata
RF	receptive field
ST	superior temporal sulcus
VM	vertical meridian
V1	primary visual area
V2	secondary visual area

made at several sites along each penetration. Alternate 40  $\mu\text{m}$  frozen sections, either coronal or parasagittal, were stained for cell bodies with cresyl violet or for myelin with either a modified Heidenhain-Woelke stain (Gattass et al., '81) or with the Gallyas method ('79).

### Unfolding of the cortical surface models and visual maps

In order to obtain a "map" of the visual topography of V1 for each animal, we unfolded the striate cortex by building a three-dimensional model at 7.5  $\times$  magnification and then unfolding it, following a procedure slightly different from the one previously described (Gattass and Gross, '81).

Since in this case the proper alignment and spacing between corresponding points in adjacent sessions were critical, we used horizontal reference needles as landmarks to align the wire-made contours, and calculated the correct size of the cross-linking pieces by trigonometry.

In reconstructing limited portions of V1, the "pencil and paper" technique with the controls described by Van Essen and Maunsell ('80) were routinely used. We introduced discontinuities in the map whenever the surface proved to be unflattenable, thus keeping the isometry in the map. An example of such a map is presented in Figure 3.

In order to evaluate the cortical distance between recording sites for the calculation of the magnification factor, the measurements were performed directly over the three-dimensional wire models.

## RESULTS

We first summarize the overall topographic organization of V1, then present evidence for the detailed topographic organization of V1. Then we illustrate the topographic changes at the borders of striate cortex. In subsequent parts of this section, we consider the cortical magnification in different portions and along different dimensions of V1. Finally, we study the variations of receptive field size and point image size with eccentricity.

### Overall organization of V1

Figure 1 summarizes the visual topography of V1 and the extent of the visual field represented in this area. In each hemisphere, V1 contains a continuous representation of the contralateral visual hemifield. The foveal representation is

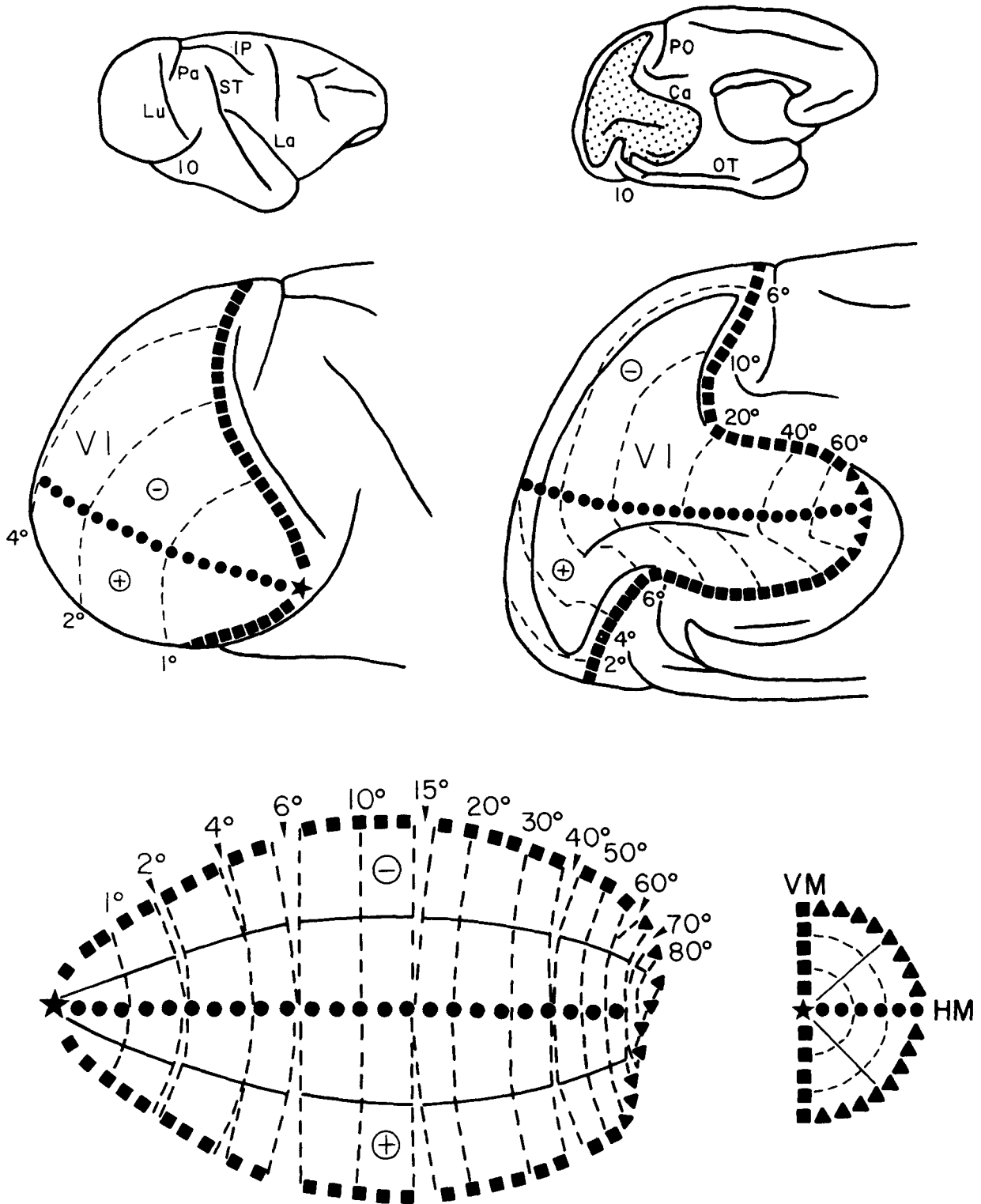


Fig. 1. Visual organization of V1. The drawings are based on photographs of a brain in which the calcarine and the collateral sulci were partially opened. Upper drawings are lateral (left) and medial (right) views of the brain showing the portions enlarged in the middle drawings. Lower drawing is a flattened map of V1 based on cortical magnification factors; the arrowheads point to the discontinuities necessary to enable flattening of the map

without distortions. The squares indicate the vertical meridian (VM), the filled circles indicate the horizontal meridian (HM), the triangles indicate the periphery, and the star indicates the center of gaze. The dashed lines are isoeccentricity lines. Insert is a representation of the visual hemifield in polar coordinates.

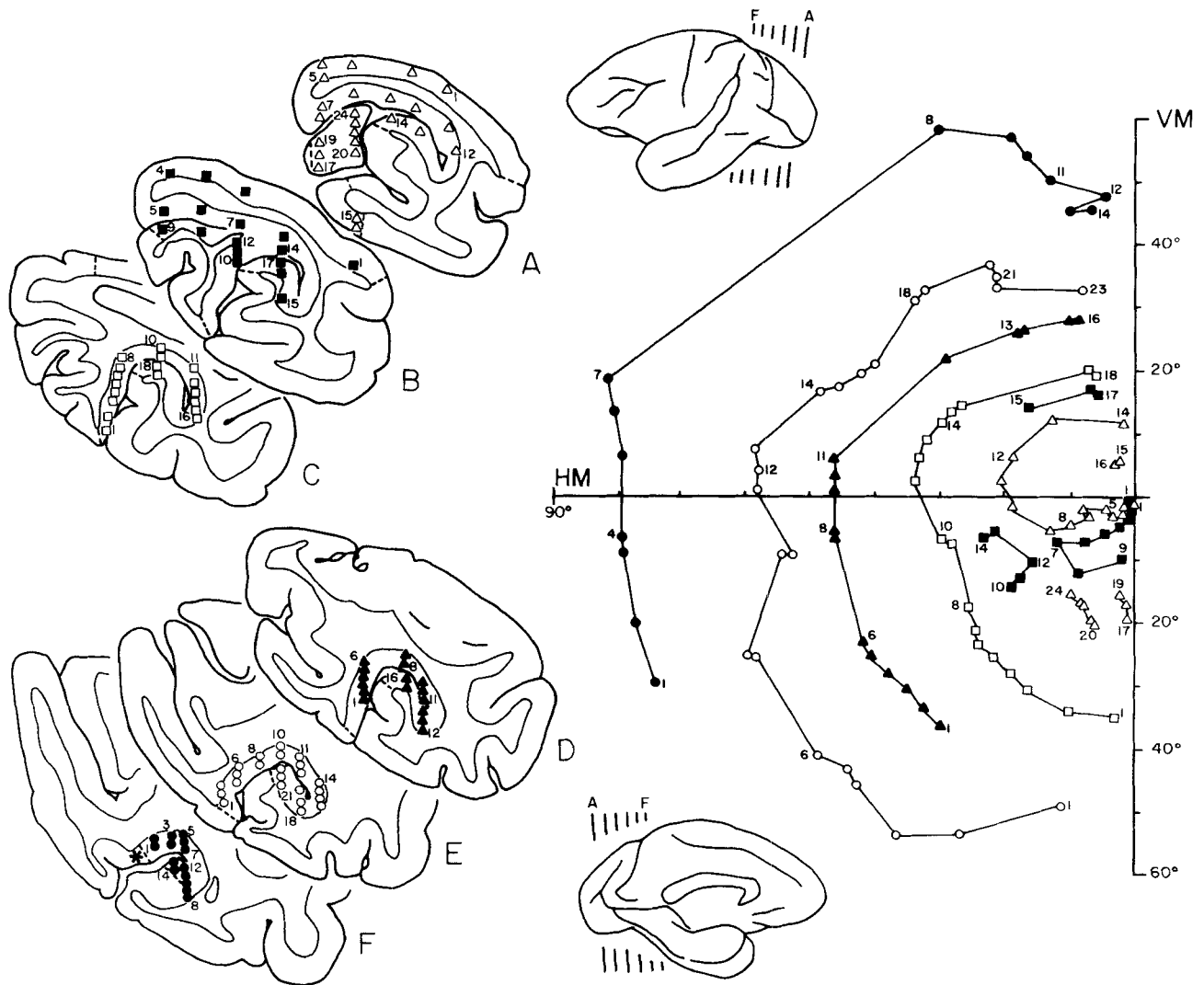


Fig. 2. Location of receptive field centers (right) in V1 corresponding to recording sites indicated in the coronal sections (A-F) cut at the levels indicated in the lateral (upper insert) and medial (lower insert) views of the brain. The dashed lines on the sections indicate myeloarchitectonic borders. The asterisk in section F indicates a recording site with no visual drive.

located ventrolaterally in the opercular surface of striate cortex, with parafoveal eccentricities up to  $5-7^\circ$  being represented posterior and medially. Beyond these eccentricities, the representation of the visual field is buried medially in the calcarine fissure. The representation of the vertical meridian forms the external border of V1 except for a small region at the anteriormost portion of striate cortex, in the calcarine sulcus, where we found a representation of the periphery. (See Figs. 1,3, 9). The representation of the horizontal meridian runs across the operculum and the calcarine sulcus dividing V1 in such a way that the representation of the lower quadrant is located dorsally and that of the upper quadrant, ventrally.

The area of V1 was estimated on three-dimensional models of striate cortex in three animals. The values obtained, for each hemisphere, were: 1025, 1049, and 1115 mm<sup>2</sup>.

Based on neuroanatomical tracer studies, we found in the *Cebus* a foveal representation of V2 anterior to that of V1 (Rosa et al., '84; Gattass et al., '84; Piñon et al., '86). V1 is bordered by V2 except for a small region at the anteriormost portion of the calcarine sulcus, where it is bordered by the area prostriata.

#### Visuotopic organization of V1

Figure 2 shows locations of receptive field centers and corresponding recording sites in coronal sections through V1 in one animal (CB 04). It summarizes the principal features of the visuotopic organization of V1. The lateral and medial surfaces of the striate area (section A, sites 1-7, 15-16; section B, sites 1-5) contain the representation of the central  $6^\circ$  of the visual field. All the visual field beyond this eccentricity is represented along the banks of the cal-

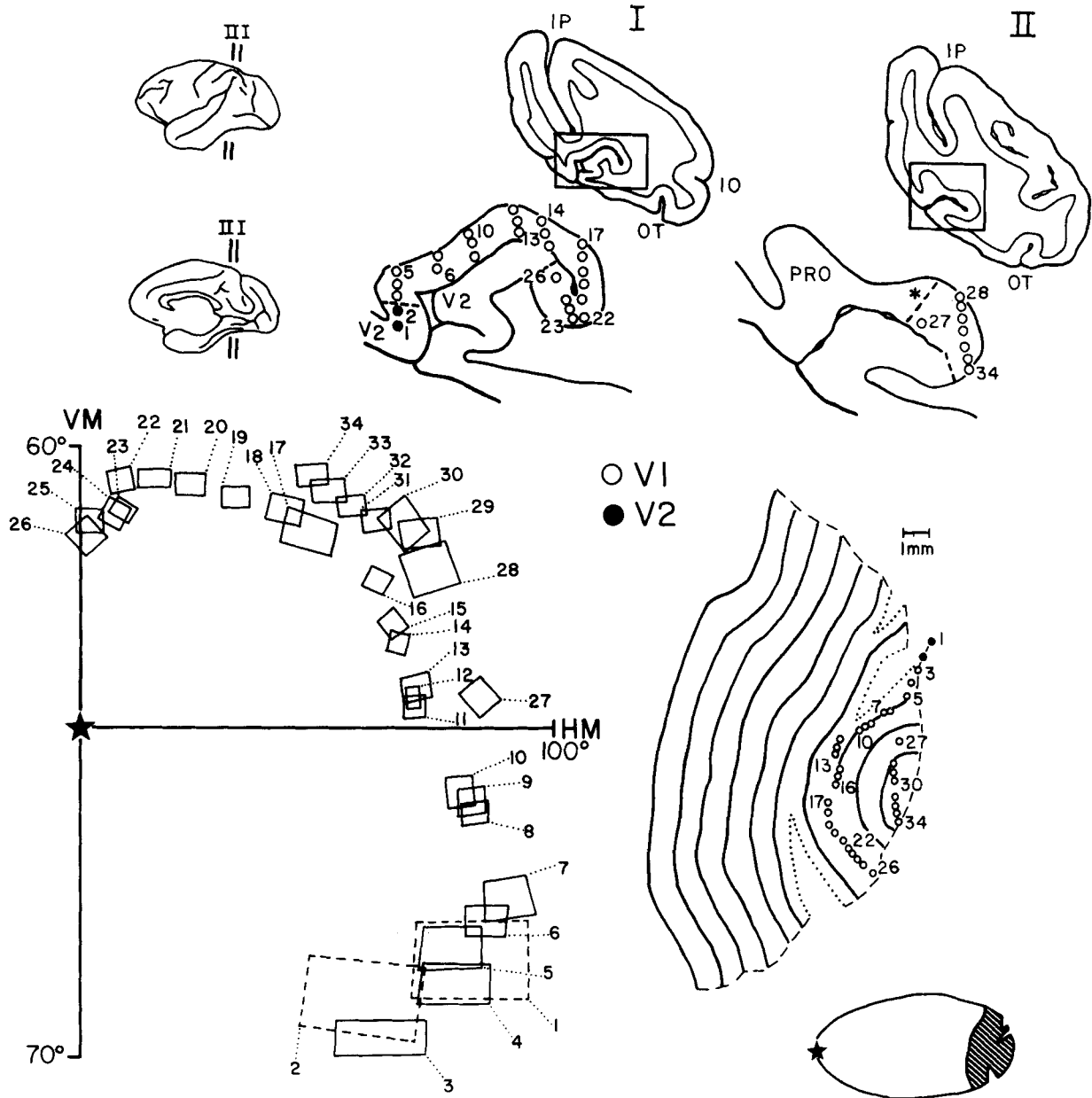


Fig. 3. Peripheral receptive fields in V1 (continuous) and V2 (dashed) corresponding to recording sites indicated in two coronal sections as shown in the lateral view of the brain. Lower right is a flattened map of the

anteriormost portion of V1 in the calcarine sulcus corresponding to the shaded area of the flattened map illustrated in the insert (bottom right). Asterisk in section II indicates a recording site with no visual drive.

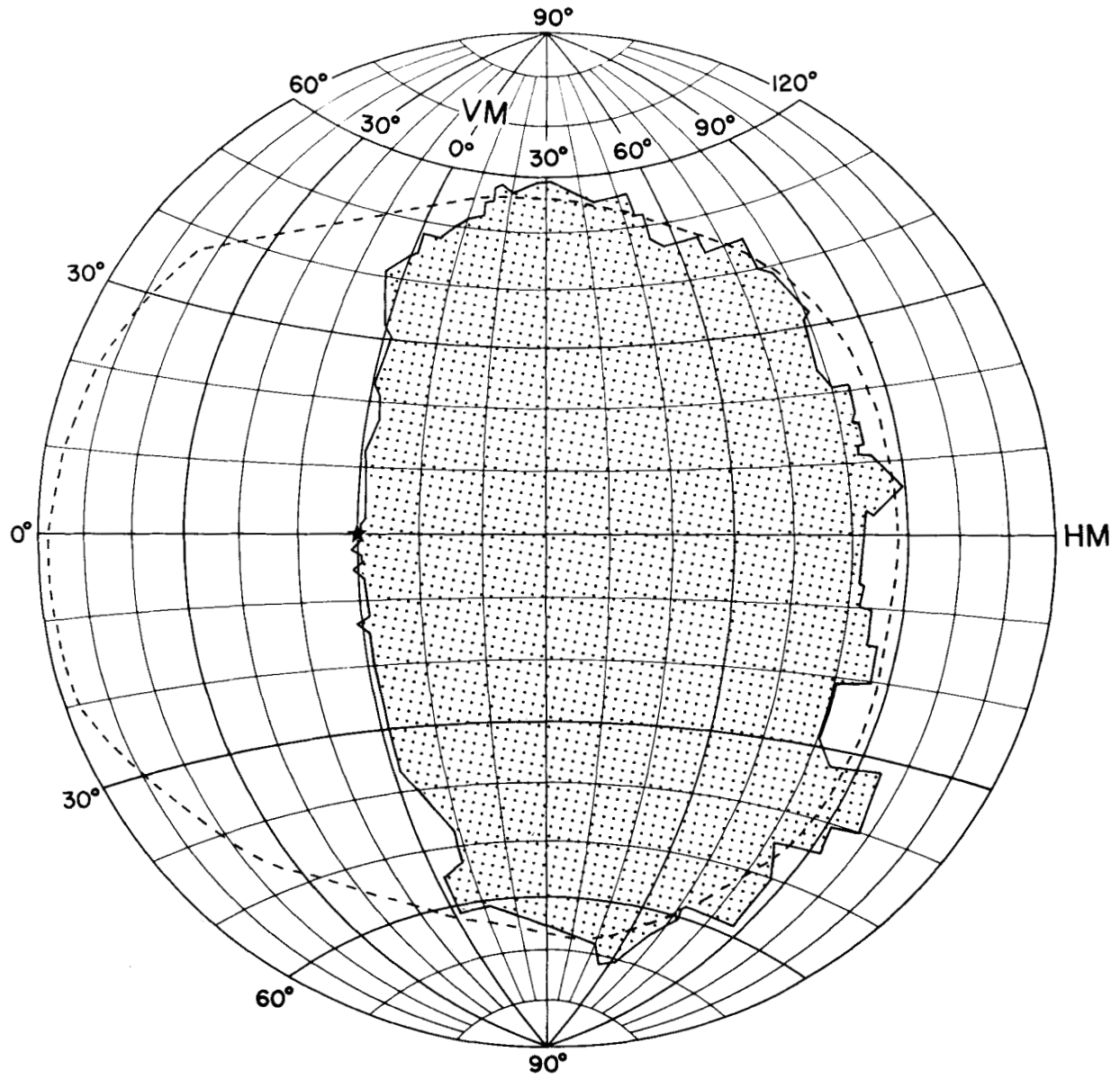


Fig. 4. Extent of the visual field represented in V1 (shaded). The dashed line indicates the extent of the visible field of vision. (Pool from nine animals).

carine sulcus. As one moves anteriorly along the banks of the calcarine sulcus, the receptive fields move progressively toward the periphery of the visual field. The extreme periphery of the visual field is represented at more anterior levels in the calcarine sulcus. Figure 3 illustrates receptive fields and corresponding recording sites in two coronal sections at the anteriormost portion of V1 in the calcarine sulcus, from a different animal. The myeloarchitectonic borders of V1 coincide with the representation of the vertical meridian except at the anteriormost portion of the calcarine sulcus where it coincides with a portion of the periphery of the lower visual field. Receptive fields corresponding to sites recorded close to the myeloarchitectonic border of V1 (Fig. 2, section F, site 1; Fig. 3, sites 3, 34) are located at the far periphery, both in the upper and lower quadrants. The representation of the horizontal meridian runs posterior and obliquely along the operculum, enters the medial surface, and then runs anteriorly along the calcarine sulcus, dividing V1 in such a way that the lower visual quadrant is represented dorsomedially in the upper bank, and the upper visual quadrant in the remaining portion of the upper bank and part of the lower bank of the calcarine sulcus, as illustrated in Figure 2.

In each hemisphere, V1 contains a representation of the contralateral hemifield with virtually no representation of the ipsilateral visual field (Fig. 4). In all animals, although receptive field borders occasionally invaded the ipsilateral hemifield, no receptive field centers were found in the ipsilateral visual field, even at more peripheral regions. The total extent of the visual field represented in V1 coincides with the field of vision of the monkey in the paralyzed condition (Fig. 4). The field of vision was inferred by plotting the limit in which the corneal reflex of a punctiform light source observed along the optical axis of the eye disappeared. Thus, the asymmetry in the representation of the visual field observed in V1, with a larger representation of the lower field, follows the asymmetry found in the periphery of the field of vision.

Figure 5 shows a summary of the visuotopic organization of V1 in a series of coronal sections spaced by 1 mm, running from the occipital pole (section A) to the anteriormost portion of the striate cortex in the calcarine sulcus (section T). Although the visual map of V1 shown in this figure is based on data from one animal, it is consistent with data from all animals.

The representation of the visual field in these sections is presented in an equatorial zenithal projection, with azimuths in dotted lines and elevations in continuous lines. The horizontal (dots) and vertical (squares) meridians, as well as the representation of the periphery (triangles), are drawn across the cortical layers, orthogonal to the cortical surface. The border between layer VI and the white matter is shown in a continuous line in V1, and in a dashed line in surrounding areas.

Figure 6 shows two flattened maps of the same animal illustrated in Figure 5; one with the contours of layer IV of the sections (A–T), and the other with the same outline but with the visual map of V1 in the equatorial zenithal coordinates projected onto it. It should be noticed that these flattened maps are somewhat distorted since, for clarity, we have chosen not to introduce discontinuities. These maps are useful to localize the representation of points of the visual field in V1. For example, a point in the upper visual field, defined by the coordinates azimuth  $10^\circ$ , elevation  $10^\circ$

(asterisk), can be located in section E by the following procedure: after localizing the point in the visual map in Figure 6 lower, we search for the corresponding site in the flattened map containing the contours of layer IV of the sections, Figure 6 upper. In this case, it corresponds to a point along the contour of layer IV in section E, between the representations of the horizontal and vertical meridians. In section E (Fig. 5), this point is found in the lower bank of the calcarine sulcus (arrowhead). Thus, it can be reached by an electrode placed at about 5 mm anterior to the occipital pole and approximately 11 mm lateral to the midline.

### Borders of V1

Abrupt changes in the sequence of receptive field centers as well as in receptive field sizes are the criteria used to delineate the electrophysiological borders of V1. These changes coincide with the cyto- and myeloarchitectonic borders of striate cortex. In most of striate cortex as we record from sites successively closer to the border of V1, the receptive field centers move toward the vertical meridian (Figs. 7–8). Crossing the border of V1, the field progression reverses and the centers move away from the VM (Fig. 7, sites 5–6; Fig. 8, sites 4–5, 20–21).

The eccentricity of the receptive-field centers corresponding to recording sites located in V1 and V2, close to the border between these areas, is similar. That is, receptive fields corresponding to recording sites in V1 and V2, which are separated by approximately 1 millimeter, partially overlap (Fig. 8). This suggests that V1 and V2 have congruent borders at the region of representation of the VM. At more anterior regions, in the upper bank of the calcarine sulcus where V1 borders V2 at the periphery, we may observe congruent or incongruent borders, as illustrated in Figure 3 (sites 2–3) and Figure 9 (sites 3–4), respectively. At the anteriormost region of the calcarine sulcus, V1 no longer borders V2; instead, it borders an area with low myelination, the area prostriata (Sanides, '72), as illustrated in Figure 15B. Under our experimental conditions, no visually driven responses were obtained in this region, although we recorded rich spontaneous activity (asterisk Fig. 2, section F; Fig. 3, section II). Receptive fields corresponding to sites located in V1 close to this border represent the far periphery of the visual field.

The topographical changes observed at the V1 border coincide with an increase in receptive field sizes, a fact that is evident both for central (Fig. 7) and for more peripheral fields (Figs. 3, 8–9).

### Cortical magnification factor

In order to verify the isotropism of the visual map of V1, we built three-dimensional models of layer IV of striate cortex to locate precisely the projection of recording sites onto the cortical surface. In these models we measured the cortical distance between recording sites to calculate cortical magnification factors in each quadrant and along the radial (isopolar) and concentric (isoeccentric) dimensions of the visual map. Figure 10 shows stereopairs of two such models at different stages of unfolding. Three-dimensional surfaces reconstructed from coronal (A) or parasagittal (B) sections are similar. These surfaces can be unfolded and everted but not flattened without introducing large areal distortions. Note in the series of stereoscopic pairs of Figure 10A that the intact model (upper) could be unfolded (middle)

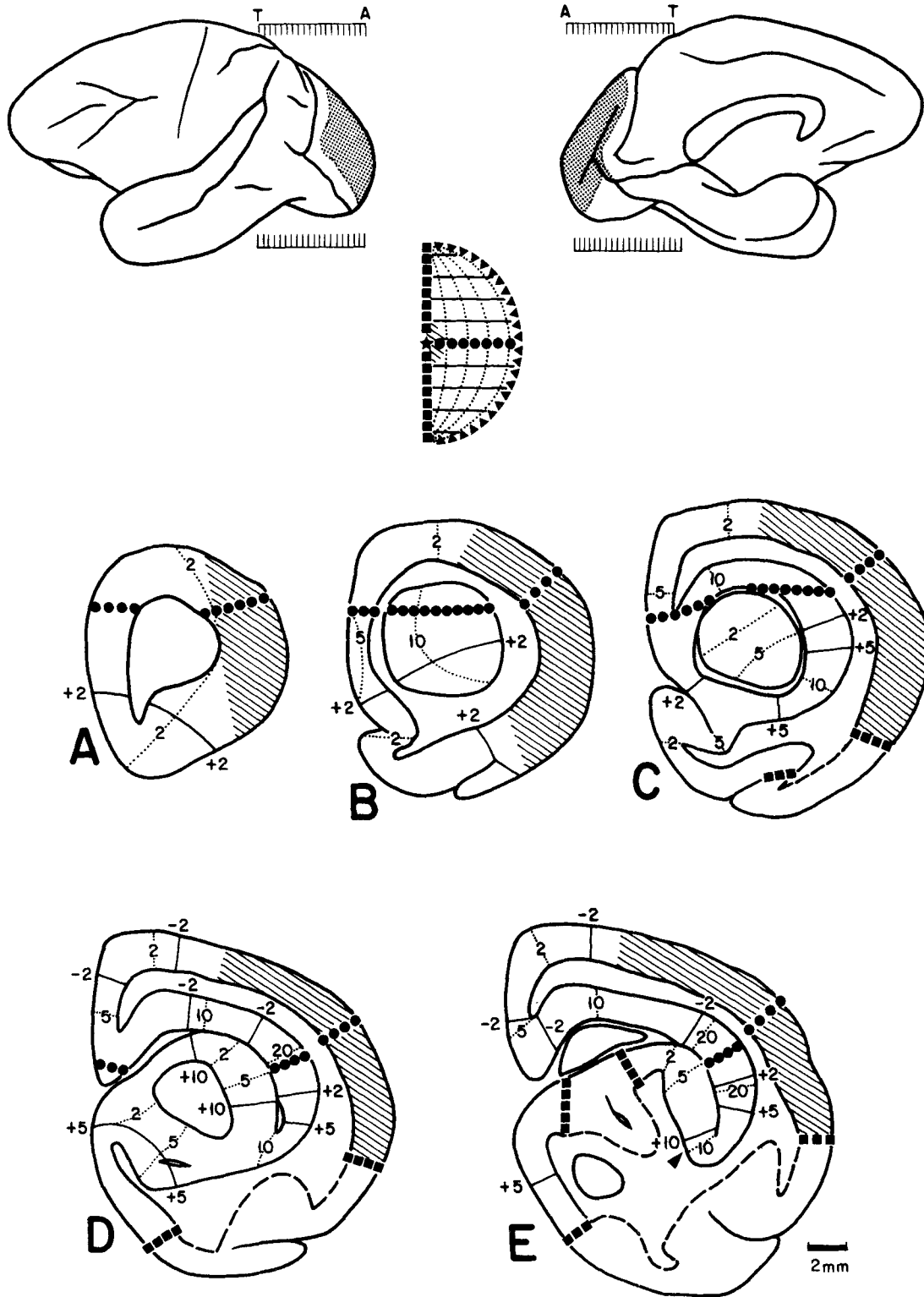


Fig. 5. Visual topography of V1 in a series of coronal sections at the levels (A-T) indicated in the lateral (left) and medial (right) views of the brain. The contralateral hemifield is represented in equatorial zenithal coordinates in the insert with azimuths in dotted lines, elevations in continuous

lines, vertical meridian in squares, horizontal meridian in filled circles, center of gaze in star, foveal representation hatched, and far periphery in triangles. (For details see text.)

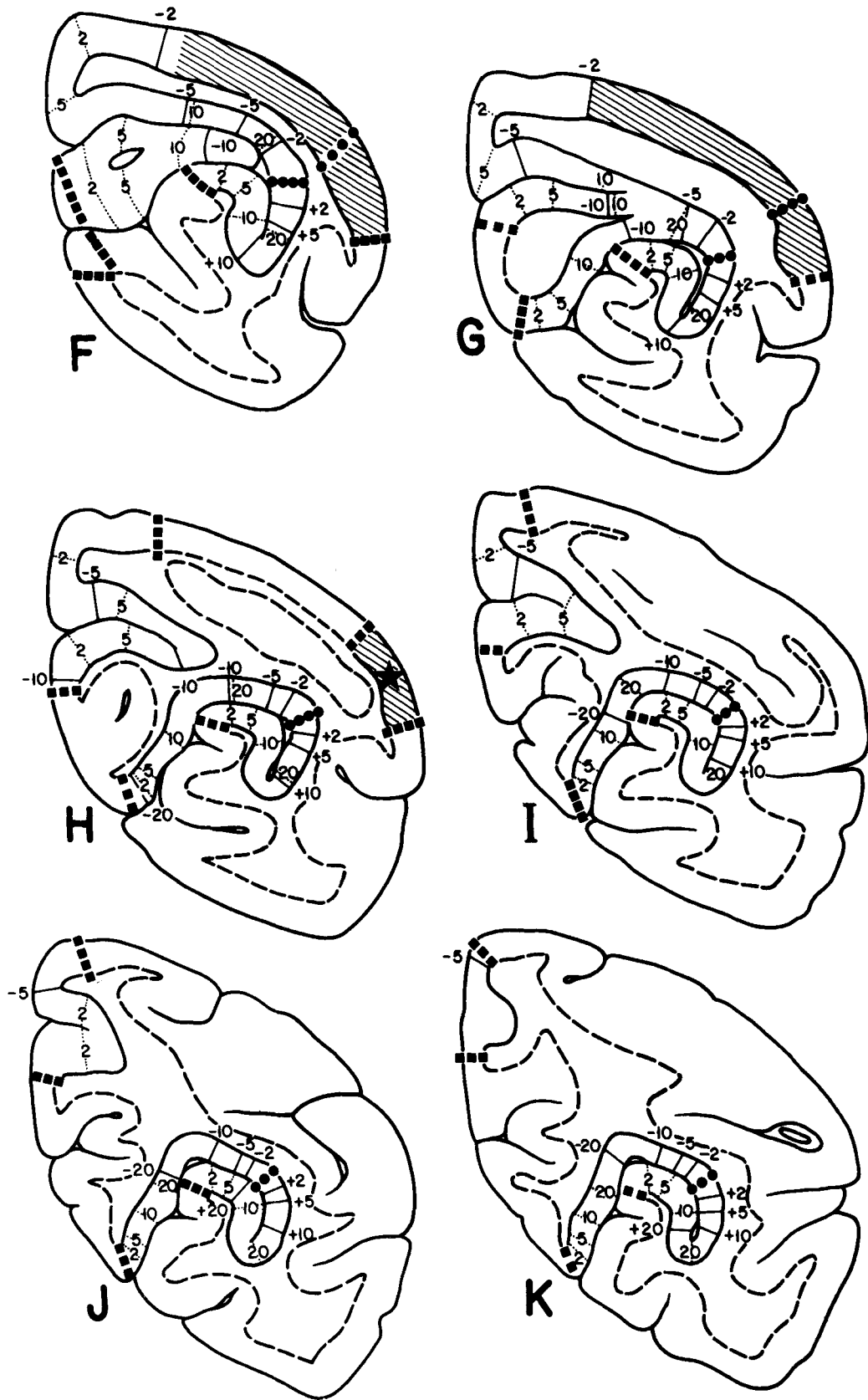


Figure 5 continued

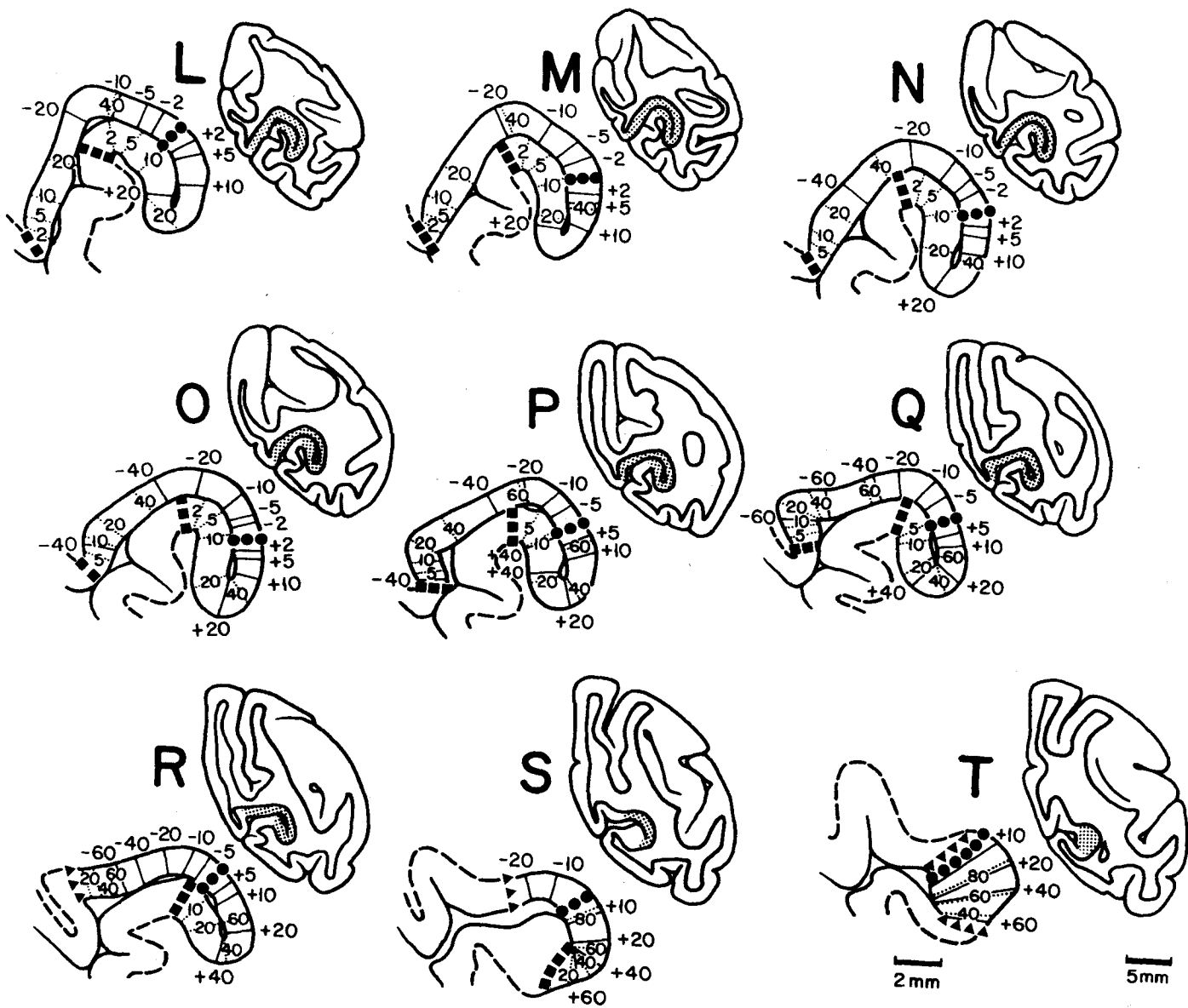


Figure 5 continued

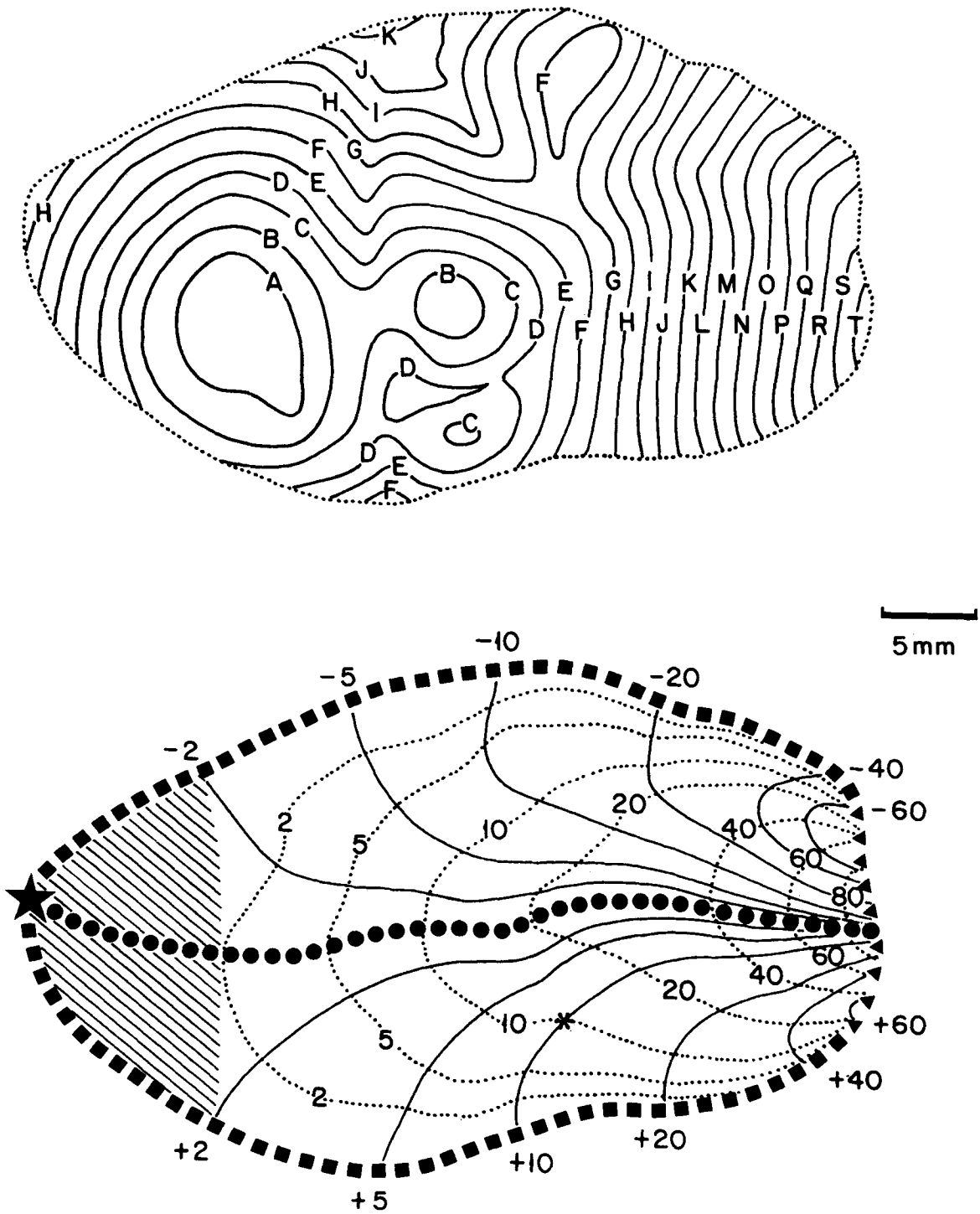


Fig. 6. Schematic flattened maps of striate cortex with the contours of the coronal sections (upper) and the map of the visual topography of V1 in equatorial zenithal coordinates (lower). (For details see text.)

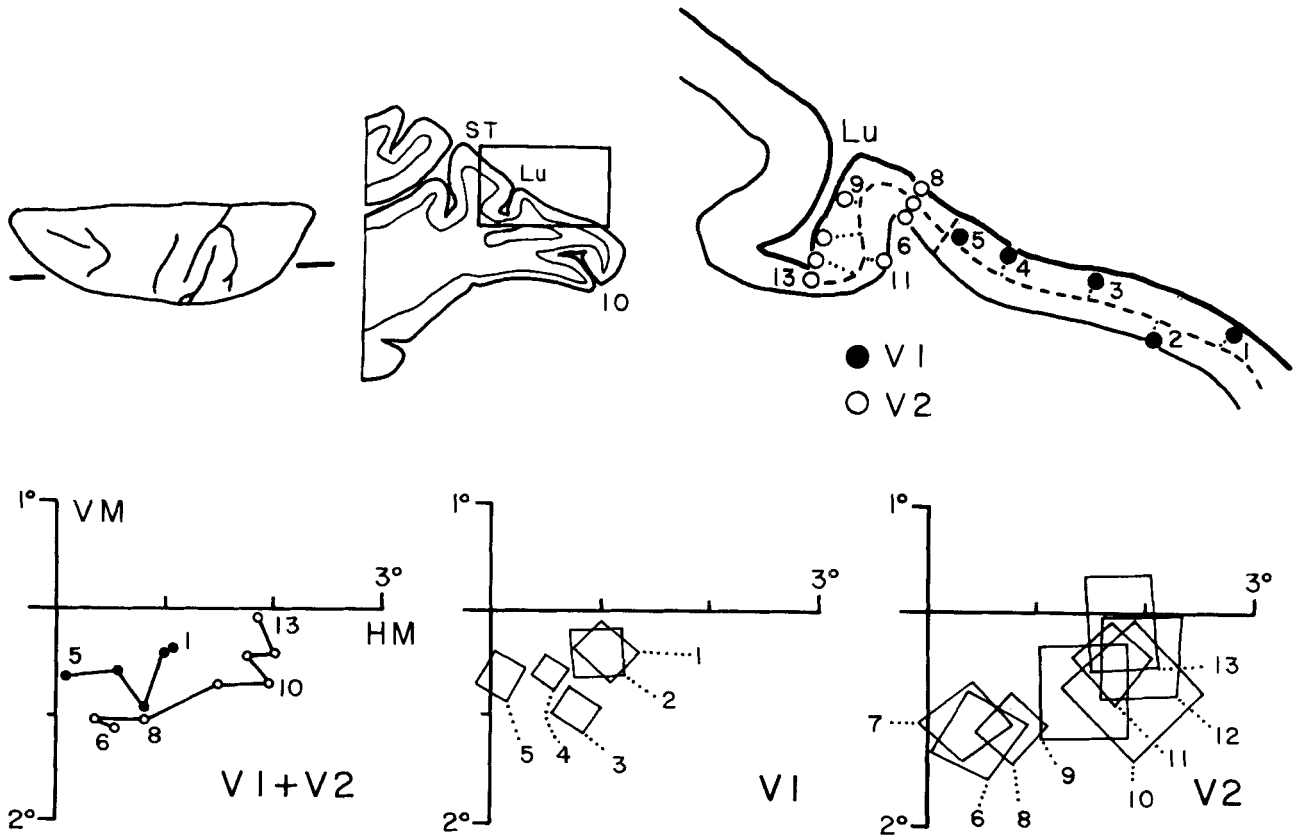


Fig. 7. Location of central receptive fields in V1 and V2 corresponding to recording sites indicated in the parasagittal section (cut at the level indicated on the dorsal view of the brain). Lower: location of receptive field centers in V1 and V2 (left), and of receptive fields in V1 (middle) and in V2 (right).

without significant surface distortion. In Figure 10A (lower) the opercular surface has been everted, allowing a better evaluation of the intrinsic curvature of V1 as a whole.

The cortical magnification factor (CMF), the ratio of the cortical distance in millimeters between two recording sites and the corresponding displacement of receptive field centers in degrees, was determined based on discrete measurements in V1 in three animals.

The CMF as a function of eccentricity (ecc) for one animal is shown in Figure 11A. The best-fitting power function (dashed line) for points between 2.0° and 70° is given by equation (1), where M = magnification, ecc = eccentricity, R = coefficient of correlation, SE = standard error.

$$M = 7.72 (ecc)^{-.94} (R = .97; SE = .24) \quad (1)$$

In order to evaluate the anisotropies in the representation of the visual field, we fitted separate power functions (dashed lines) to the data measured along isoeccentric (Me) (Fig. 11B) and isopolar (Mp) (Fig. 11C) dimensions. The corresponding equations (2) and (3) are statistically different ( $p < 0.005$ ;  $t$  of the slope = 2.85), a result that supports the concept of an anisotropic map.

$$Me = 7.41 (ecc)^{-.97} (R = .98; SE = .22) (n = 87) \quad (2)$$

$$Mp = 7.69 (ecc)^{-.88} (R = .98; SE = .17) (n = 82) \quad (3)$$

A close inspection of the distribution of the data with respect to the regression lines (1-3) reveals, however, that a power function may not be the best-fitting function for the data. After testing other types of regressions, we obtained higher coefficients of correlation and lower standard errors with second-order polynomial functions to the natural logarithms of CMF and eccentricity (continuous lines Fig. 11), expressed in equations (4) to (6).

$$\begin{aligned} \ln(M) &= 1.45 - .35 [\ln(ecc)] - .12[\ln(ecc)]^2 (R \\ &= .98; SE = .22) \quad (4) \end{aligned}$$

$$\begin{aligned} \ln(Me) &= 1.36 - .31 [\ln(ecc)] - .13[\ln(ecc)]^2 (R \\ &= .99; SE = .18) \quad (5) \end{aligned}$$

$$\begin{aligned} \ln(Mp) &= 1.69 - .56 [\ln(ecc)] - .07[\ln(ecc)]^2 (R \\ &= .98; SE = .16) \quad (6) \end{aligned}$$

We also studied the functions for Mp and Me values from two other animals. The difference between Mp and Me values in the periphery, beyond 30°, was also observed in these animals. Thus, the Mp/Me anisotropy may be a constant feature of the peripheral field representation in V1.

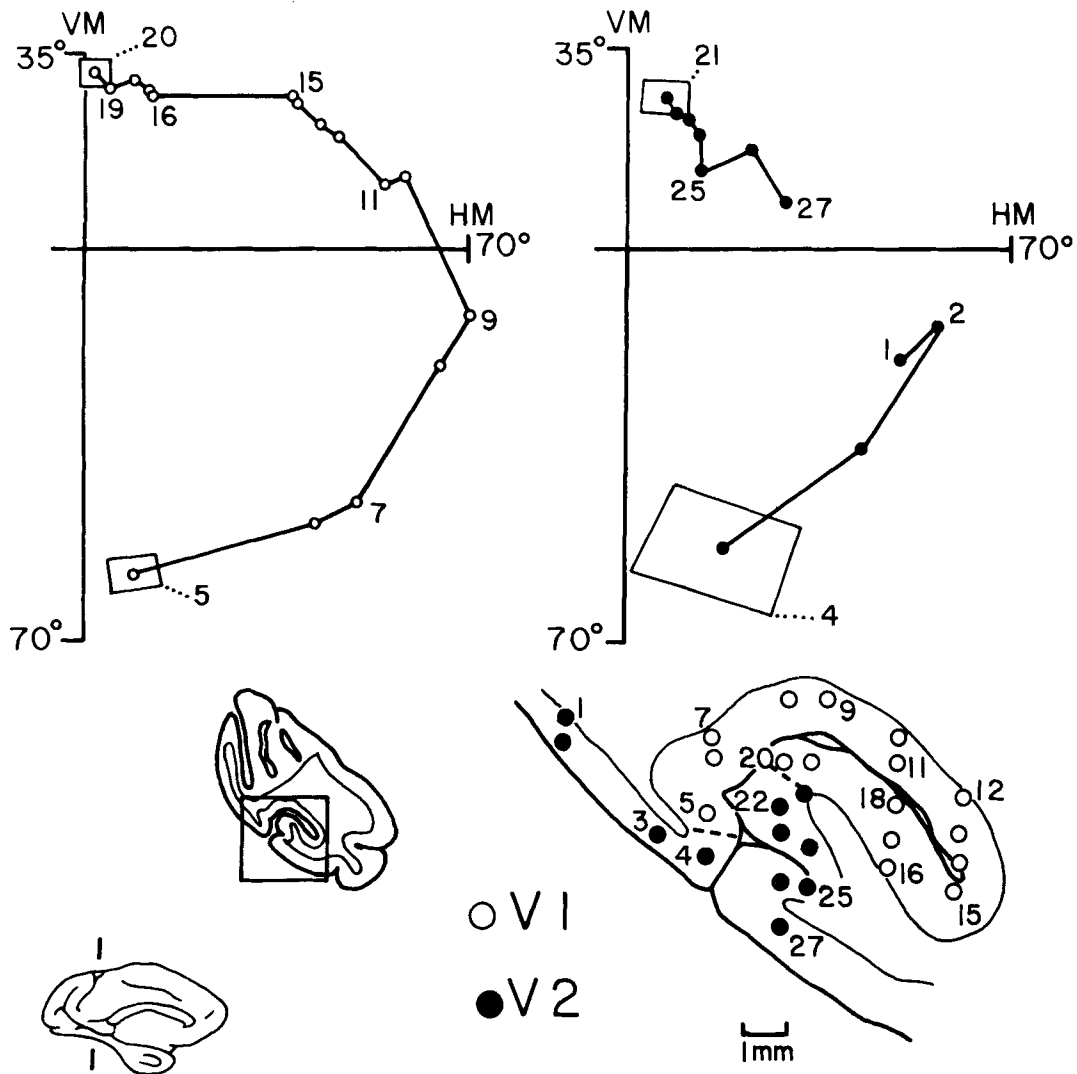


Fig. 8. Location of peripheral receptive field centers in V1 (left) and V2 (right) corresponding to recording sites indicated in the coronal section, cut at the level indicated in the medial view of the brain.

The areal cortical magnification factor (ACMF), the relationship between a cortical surface in square millimeters and the area of the corresponding segment of the visual field in square degrees, was also studied in the animal that yielded equations (1) to (6). Isoeccentric and isopolar contours were used to delimitate 57 small segments in the cortical map. These segments were transferred from the three-dimensional model of V1 to translucent plastic sheets and then to a flat surface. The segments were made small enough to minimize areal distortions due to intrinsic cortical curvature. We avoided using regions of low recording site densities, as well as the region of foveal representation.

The best-fitting power function relating the ACMF to eccentricity is expressed in equation (7).

$$ACMF = 60.65 (ecc)^{-1.88} (R = .99; SE = .23) \quad (7)$$

In theory, the mean CMF for a given eccentricity is the square root of the ACMF. This relation was confirmed in this animal since the square root of the ACMF was shown not to be statistically different from CMF ( $t$  of the slope = .67;  $.5 < p < .55$ ;  $t$  of the intercept = .26;  $.75 < p < .8$ ). The values of the square root of ACMF corresponding to the 57 segments studied in four sectors of the visual hemifield are shown in Figure 12. Equation (8) relates the square root of ACMF to eccentricity; the corresponding power function is shown in Figure 12 (dashed line). The comparison of this equation with equation (1) reveals the similarity of both the constant and the exponent of these equations.

$$Sqr(ACMF) = 7.79 (ecc)^{-.94} (R = .99; SE = .11) \quad (8)$$

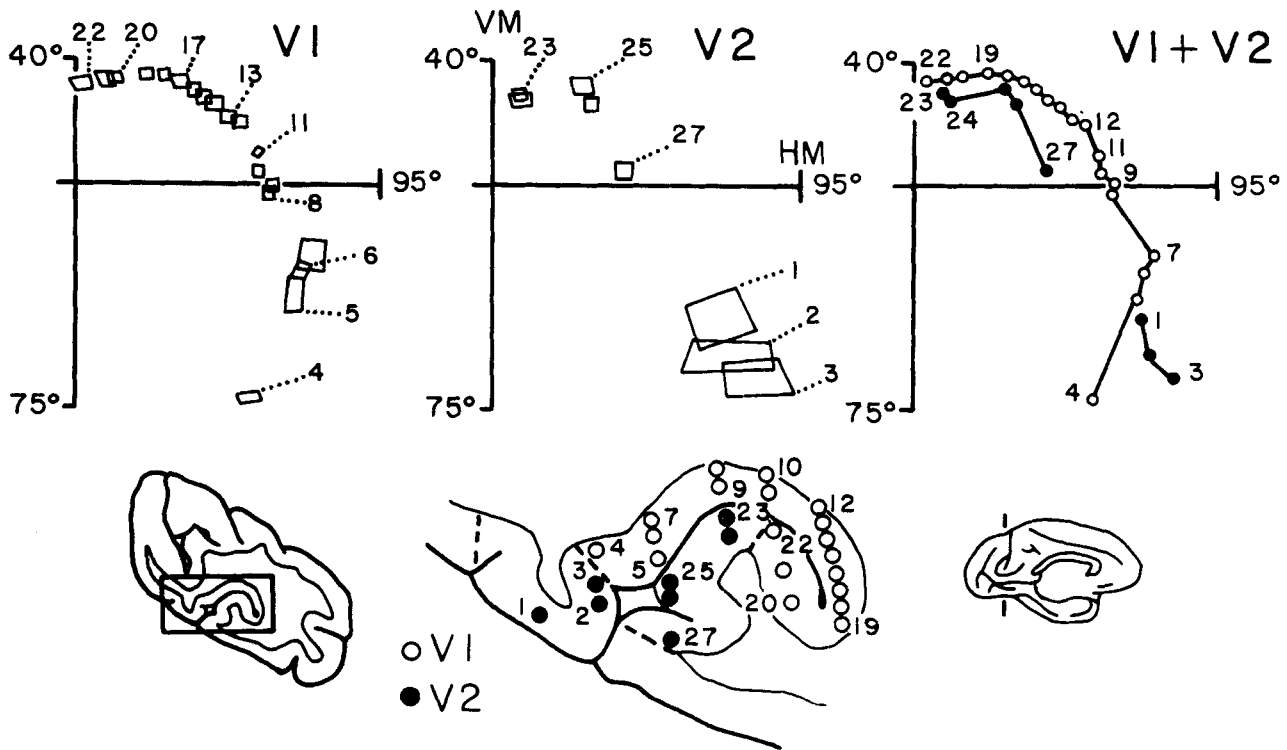


Fig. 9. Location of far peripheral receptive fields in V1 (upper left) and V2 (upper middle) corresponding to recording sites indicated in the coronal section. Upper right: location of the corresponding receptive field centers.

As observed for the cortical magnification function, a lower standard error and higher coefficient of correlation are obtained by fitting a second-order polynomial function (Fig. 12, continuous line) to the natural logarithms of both Sqr(ACMF) and eccentricity:

$$\text{Ln}[\text{Sqr}(\text{ACMF})] = 1.59 - .49 [\text{Ln}(\text{ecc})] - .09 [\text{Ln}(\text{ecc})]^2 \quad (R = .99; \text{SE} = .09) \quad (9)$$

As shown in Figure 12, we were unable to detect any systematic differences in the ACMF values, for the various sectors of the visual field. In particular, we have no evidence for a lower magnification of the upper visual field representation when compared to that of the lower visual field, although in this animal, we had no data below 10° in the upper visual field. However, direct measurements of the cortical surfaces devoted to the representation of both quadrants confirm this point. For example, in this animal, which has a V1 with 1115mm<sup>2</sup>, the area of the lower visual field representation between 2° and 47° eccentricities is 498.3 mm<sup>2</sup>, whereas the corresponding region in the upper visual field is 488 mm<sup>2</sup>.

**Receptive field size and cortical point image size vs. eccentricity**

The variation of multiunit receptive field size (i.e., the square root of the receptive field area) with eccentricity in

V1 in *Cebus* is shown in Figure 13. The data obtained from nine animals are shown in a double-logarithmic plot. Close observation of the data distribution shows that our sample included a greater number of peripheral receptive fields, with few receptive fields located within the central 10°. The centralmost fields (those below 5°) were recorded shortly after projecting the center of the fovea onto the hemisphere, in an attempt to reduce errors in the location of the center of the receptive fields due to slow eye movements.

Two equations were calculated to describe the relation of field size with eccentricity. The best linear function obtained is shown in equation (10):

$$\text{Sqr}(\text{RF Area}) = .83 + .06 (\text{ecc}) \quad (10)$$

As shown in Figure 13 (dashed line), this function describes our data well, except for the centralmost receptive fields, which are overestimated. A better fit was obtained by applying a second-order polynomial (equation 11) to the natural logarithms of both receptive field size and eccentricity (Fig. 13, continuous line):

$$\text{Ln}[\text{Sqr}(\text{RF area})] = -.56 + .25 [\text{Ln}(\text{ecc})] + .06 [\text{Ln}(\text{ecc})]^2 \quad (11)$$

The size of the cortical region activated by a punctiform stimulus, i.e., the point image size (McIlwain, '76), was

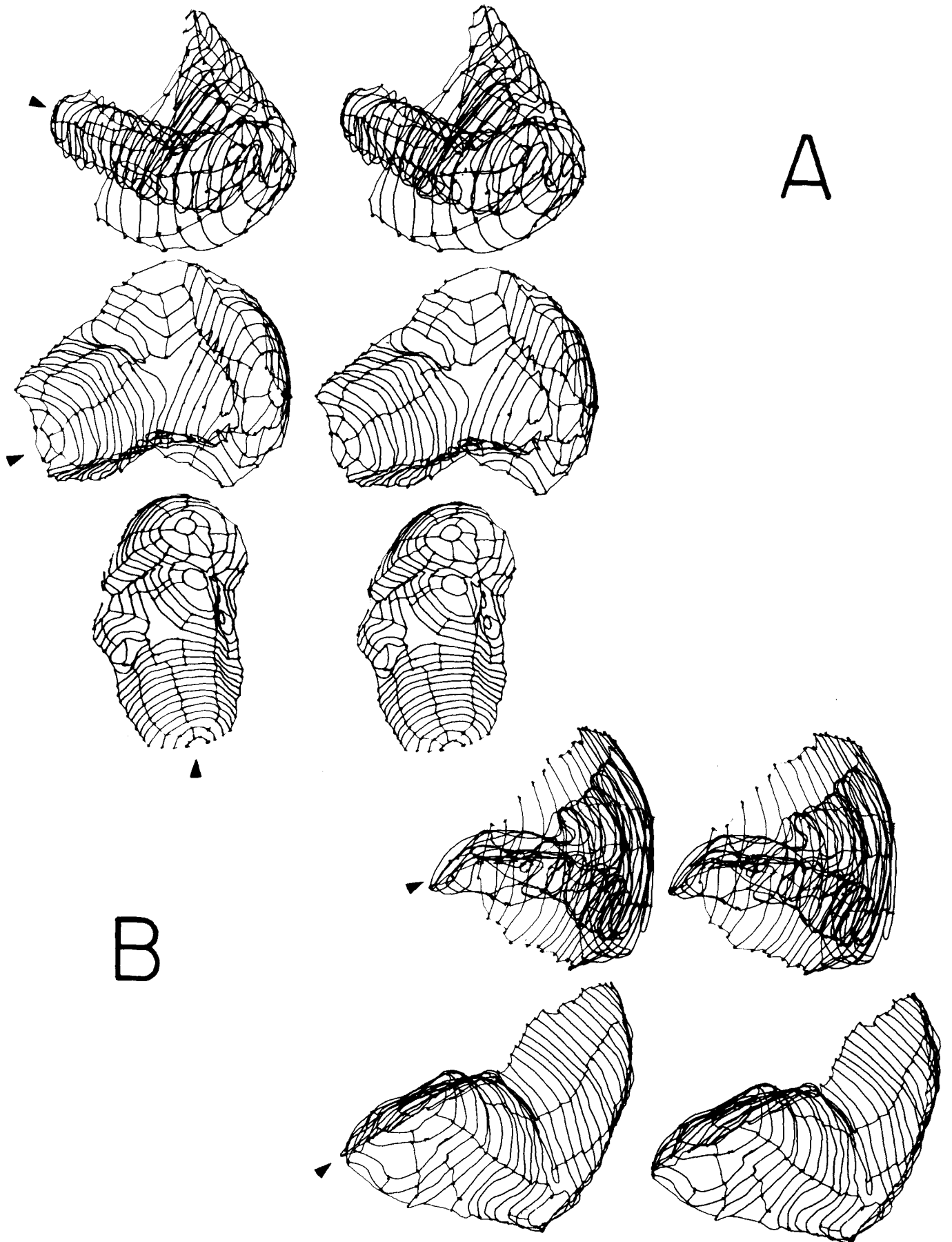


Fig. 10. Series of stereopairs (6 diopters) of three-dimensional models of V1 at different stages of unfolding. A. Model constructed from coronal sections. B. Model constructed from parasagittal sections. Arrowheads indicate the anteriormost portion of the calcarine sulcus.

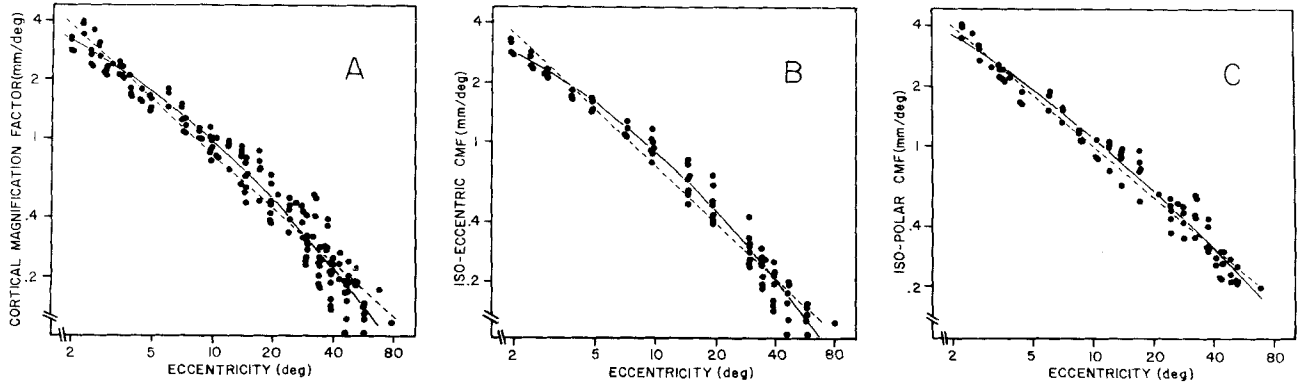


Fig. 11. A. Cortical magnification factor as a function of eccentricity for one animal. B. Cortical magnification along the isoeccentric dimension. C. Cortical magnification along isopolar dimension. The data for B and C are from the same animal illustrated in A. (For details see text.)

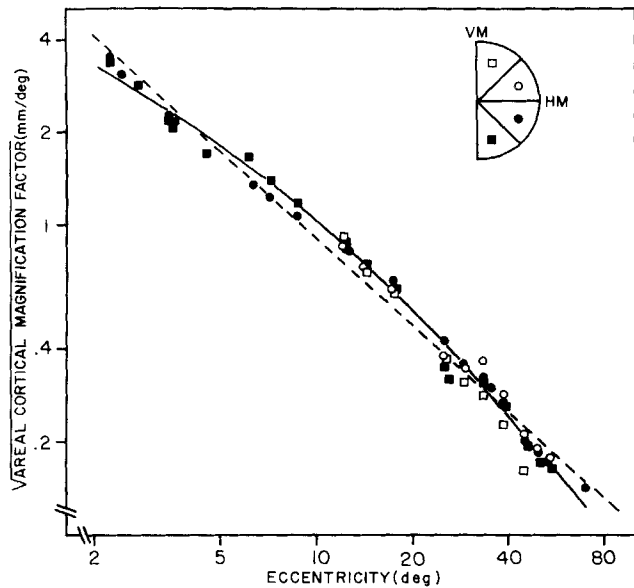


Fig. 12. Square root of the areal cortical magnification factor as a function of eccentricity for the same animal illustrated in Figure 11. Insert: representation of the visual hemifield divided in four sectors. (For details see text.)

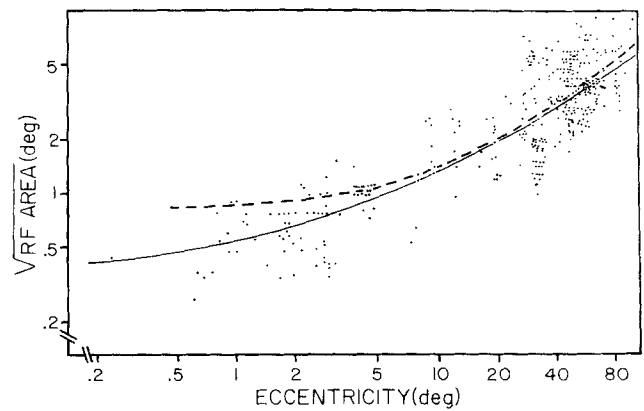


Fig. 13. Receptive field size as a function of eccentricity of receptive field center in nine animals. (For details see text.)

estimated by multiplying the cortical magnification factor by the receptive field size at various eccentricities. Figure 14 shows the variation of point image size with eccentricity.

### DISCUSSION Visuotopic organization

The main features of the visuotopic organization of V1 in the *Cebus* are similar to those reported in other primates. Except for some details, the organization in the *Cebus* is similar to that of the *Macaca*.

It has been reported in both the owl monkey (Allman and Kaas, '71) and macaque monkey (Van Essen et al., '84) that V1 is bordered by the second visual area (V2) for most of its extent, except for a small region in the anteriormost part

of the calcarine sulcus where V1 is bordered by area prostriata (Sanides, '72). Electrophysiological recordings in both species have suggested that the border between V1 and V2 is always coincident with the vertical meridian representation. In the regions where the border of V1 coincides with the representation of the visual field periphery, the neighboring area would no longer be V2; instead, it would be the area prostriata as suggested by Sanides ('72).

Our results are not in entire agreement with this interpretation. We have observed cases in which V1 borders V2 anteriorly, not in the region of representation of the vertical meridian. In these cases the border between V1 and V2 is the representation of the peripheral visual field (see Figs. 3, 9). The myeloarchitectonic borders (arrowheads) of V1 with V2 and with the area prostriata at the anteriormost portion of the superior bank of the calcarine sulcus, in one animal, are illustrated in Fig. 15A, B, respectively. In these Heidenhain Woelke stained sections, V2 is characterized by a rich band of fibers extending from layer VI to the bottom of layer III, whereas the area prostriata presents a pale myeloarchitectonic pattern as described by Sanides ('72). Figure 15C shows the section illustrated in Figure 9, stained

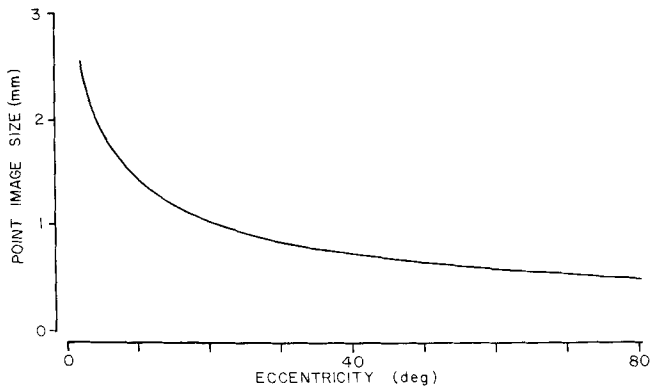


Fig. 14. Point image size as a function of eccentricity based on data from one animal.

for myelin, passing through the calcarine sulcus at a level corresponding to that of the section illustrated in Figure 15A. A close inspection of these sections shows that, at this level, V1 is bordered by V2. Thus, at least in some animals, V1 touches V2 in a region of representation of the visual field periphery.

In the paralyzed condition, the field of vision—based on the observation of the corneal reflex of the Purkinje image—coincides fairly well with the extent of the visual field obtained by plotting the external borders of the peripheral-most receptive fields recorded at the borders of V1 (see Fig. 4). In the animal shown in Figure 3, the receptive fields were recorded at the peripheral border of V1, and their sizes are compatible with the function relating receptive field size with eccentricity for V1. In addition, the magnification in this region is compatible with the values predicted by the CMF function of V1. This result is somewhat amazing since it implies either in compression or in absence of representation of parts of the retina in striate cortex. Thus, the data in this animal are inconsistent with a regular representation of the part of the visual field hidden by the orbital ridge.

### Three-dimensional nature of V1

In recent years, a great amount of data on the visuotopic organization, connections, and columnar arrangement of the visual cortex has been obtained by using various cortical "flattened map" techniques (Van Essen and Maunsell, '80; Gattass et al., '86; Le Vay et al., '85; Shipp and Zeki, '85). These bidimensional reconstructions reveal several features of the cortical organization not apparent from the study of single or even serial sections. We have thus set out to obtain similar maps from the striate cortex of the *Cebus* monkey that would, in principle, make easier the study of such features as cortical magnification and interanimal variability. We have tried to use the "pencil and paper" technique described by Van Essen and Maunsell ('80), which proved to be inadequate in this case. No arrangement of layer IV drawings as projected to a plane was obtained that could avoid severe linear and angular distortions without introducing discontinuities (see Le Vay et al., '85). Although some regions, such as most of the opercular surface, could be mapped without more than 5% distortion, other regions presented 35% of linear distortion even in the best

configuration we could obtain, as evaluated by the "test square" method described by Van Essen et al. ('84).

We have overcome this problem by generating three-dimensional models of the entire striate cortex as shown in Figure 10. Based on the locations of the recording sites and of the corresponding receptive fields, the visual maps of V1 were reconstructed onto these models. In view of the curvature shown in the series of stereoscopic pairs in Figure 10, it is clear that no disposition of the section contours would be good enough to produce a continuous and isometric map.

### Magnification factors in V1

In order to quantify the eccentricity-dependent transformation of the visual field representation in striate cortex, Daniel and Whitteridge ('61) determined, at different eccentricities, a parameter that they referred to as Cortical Magnification Factor (CMF). CMF corresponds to the cortical distance between two points, in millimeters, divided by the distance in the visual field between the centers of the corresponding receptive fields, in degrees.

Previous studies in macaque (Daniel and Whitteridge, '61), vervet (Guld and Bertulis, '76), and owl monkeys (Myerson et al., '77) have shown that in V1 the CMF decreases with increasing eccentricity following approximately a negative power function.

Several authors have investigated the variations of CMF with eccentricity in Old World monkeys. Figure 16 compares functions fitted by the method of least squares to our data in the *Cebus* and to data from previous studies in Old World monkeys (Dow et al., '81; Tootell et al., '82; Van Essen et al., '84). These functions are rather similar and have several intersecting points among them. Thus, the cortical magnification function in diurnal Old World and New World monkeys of similar size is not different.

Although no quantitative data are currently available for the cortical magnification in the *Aotus*, the comparison of the visual maps of V1 of the *Cebus*, *Macaca* (Van Essen et al., '84), and *Aotus* (Allman and Kaas, '71) reveals a clear difference in the representation of central vision. About half of the cortical surface of V1 is devoted to the central 10° both in the *Cebus* and in the *Macaca*, whereas about half of V1 in the *Aotus* is devoted to the central 20–30°. Thus, the difference in cortical magnification in these monkeys seems to be related to their habits and not to their phylogenetic roots.

It would be interesting to compare the relative emphasis of the central vision representation in diurnal Strepsirhine primates (such as *Lemur catta*) with that in diurnal monkeys. A similar emphasis in diurnal Strepsirhine primates, not present in nocturnal ones (such as *Galago*), would extend our conclusions on the role of diurnal habits in determining cortical magnification to all primates, not only to simians.

The magnification factor was not systematically studied in the foveal representation. Thus, we cannot assign precise values of areal cortical magnification factor (ACMF) to specific eccentricities below 2°. However, equation (9) predicts a surface of 132.8 mm<sup>2</sup> for the representation of eccentricities between 4 and 120 minutes, a value that is in close agreement to the one measured in the three-dimensional model for the whole foveal representation (135.4 mm<sup>2</sup>). In the absence of direct measurements within the fovea, the extrapolated values of foveal ACMF is only an estimate.

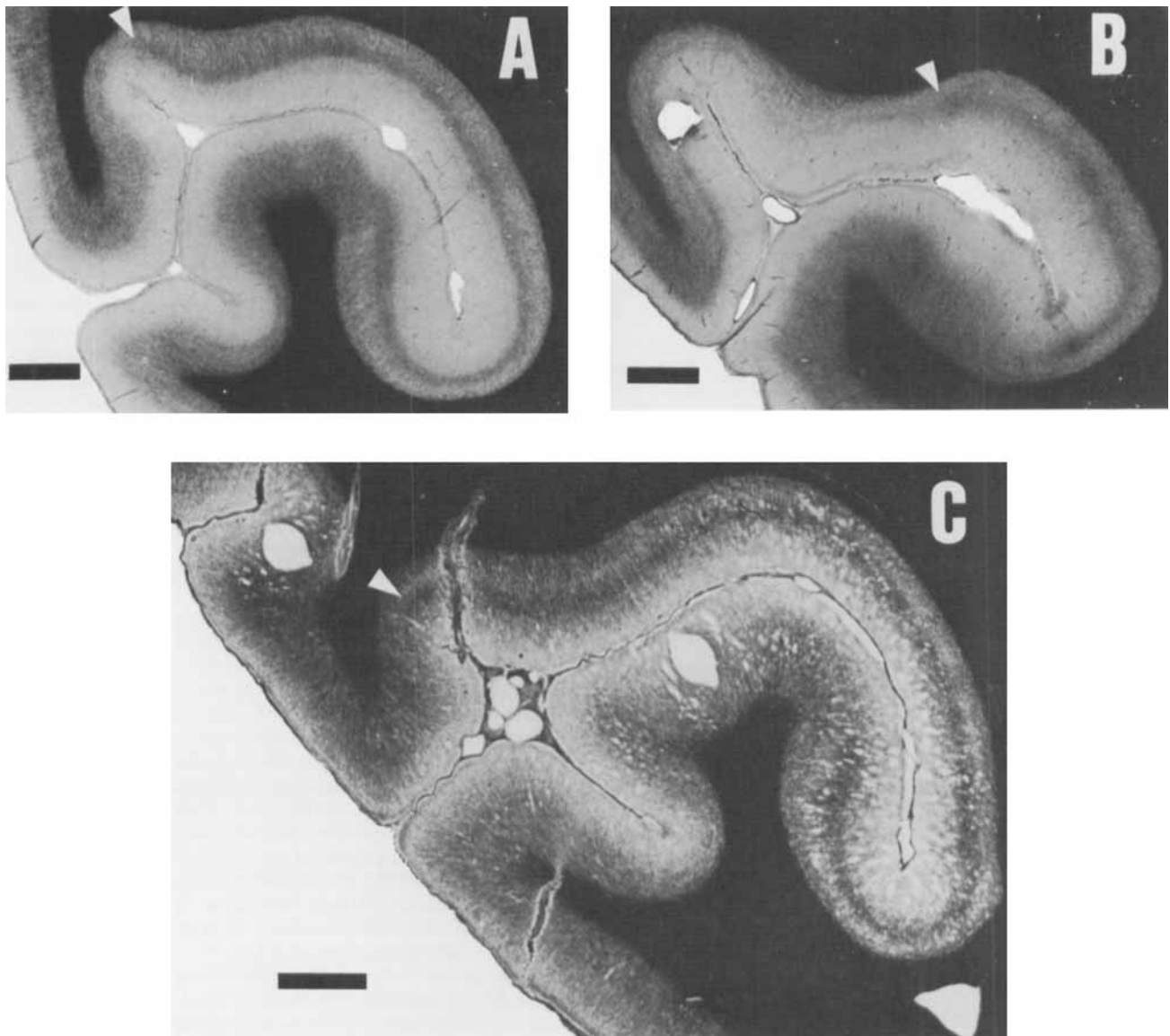


Fig. 15. Photomicrographs of myelin-stained sections through the calcarine sulcus. A and B. Heidenhain-Woelke stain. C. Gallyas' stain. Arrowheads point to the borders between V1 and V2 in A and C; and between V1 and area prostriata in B. Bars = 1 mm. In C, three electrode tracks are visible.

The maximum  $Sqr(ACMF)$  value (9.6 mm/deg at 3.95 minutes) given by this equation is a reasonable estimate of the peak CMF within foveal striate cortex. Alternatively, if we assume that the CMF variation follows a power function, and if we add a constant to the eccentricity term in equation (8) in order to match the predicted value of the area of the foveal representation to its measured value, we would obtain the equation (12), which predicts a peak CMF of 12.16 mm/deg.

$$Sqr(ACMF) = 7.79 (ecc + .62)^{-.94} \quad (12)$$

Both values are in agreement with the peak CMF (9–14.1 mm/deg.) proposed by Dow et al. ('85) for the *Macaca fascicularis*.

### Anisotropic visual map of V1

We have investigated the CMF as a function of eccentricity, using only data from regions of high recording site densities, in three animals. The cortical distances and the areal measurements were done directly on the three-dimensional models, in order to avoid local distortions induced by the cortical flattening methods in V1.

In the *Cebus*, we have not seen any difference in the magnification of the upper visual field when compared with that of the lower visual field, as reported in macaque monkeys (Van Essen et al., '84). No difference was found in areal measurements of the cortical surfaces devoted to equal portions of the visual fields in both quadrants. In the macaque, several authors (Tootell et al., '82; Van Essen et al.,

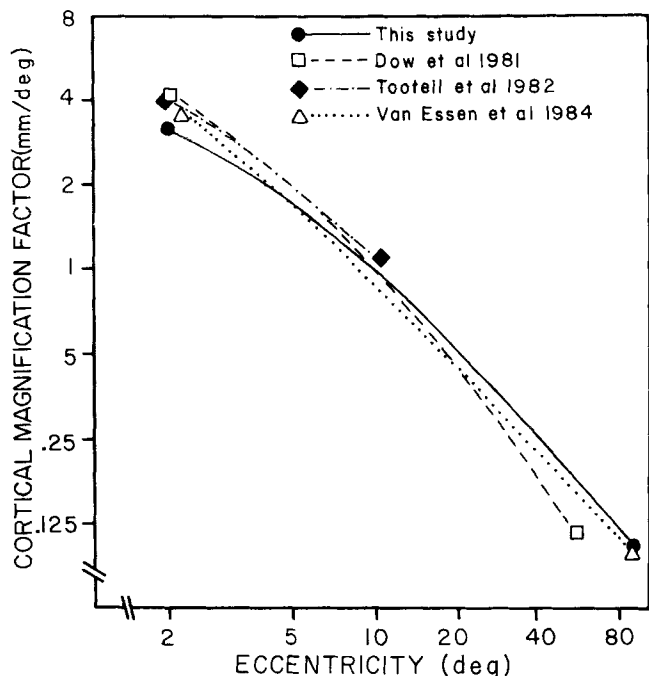


Fig. 16. Comparison of regressions of cortical magnification factor vs. eccentricity for a diurnal New World monkey (this study) and Old World monkeys (other studies).

'84) have shown that the CMF at a given eccentricity could vary depending on the direction along which the measurements were performed. This difference would produce an anisotropic representation of the visual field in V1. We have also found a difference in the magnification measured along isopolar and isoeccentric dimensions in the visual map of V1. This difference is similar to that described for the macaque (Van Essen et al., '84). The anisotropy in the visual map in the macaque has been correlated with the organization of the ocular dominance columns in V1 (Tootell et al., '82). Although no evidence for ocular dominance columns in V1 of *Cebus* exists to date, the magnitude of the anisotropy of the visual map is similar in both monkeys.

#### Point image size in V1

The function relating point image size with eccentricity was obtained by multiplying the cortical magnification factor by the corresponding multiunit receptive field size at various eccentricities.

In agreement with the results obtained in macaque monkeys (Dow et al., '81; Van Essen et al., '84), the point image size in V1 of *Cebus* varies with eccentricity. However, the function obtained in this study is similar to that proposed by Dow et al. ('81), being greater at central visual field representation, and is different from that proposed by Van Essen et al., '84 (see Fig. 17). This discrepancy is probably related to differences in the estimate of receptive field size rather than to differences in the organization of V1 in these animals. Van Essen et al. ('84) have shown that the function relating receptive field area with eccentricity for fields located between fixation and 5° is different from that obtained for fields located beyond this eccentricity. This difference, which is responsible for the biphasic nature of

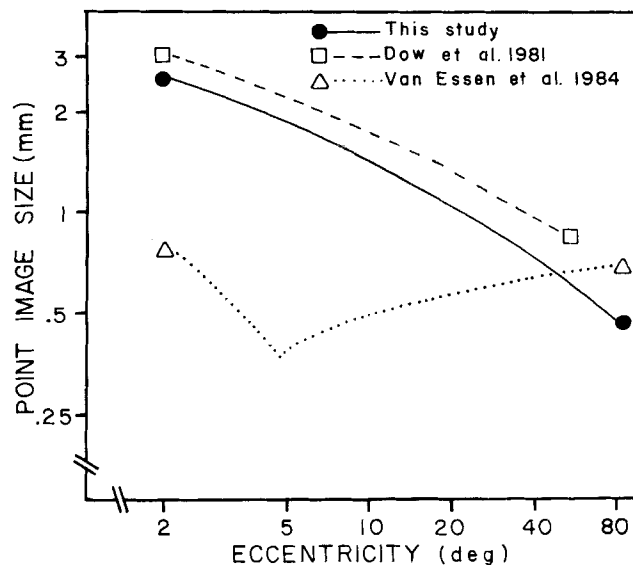


Fig. 17. Comparison of the functions obtained for point image size in *Cebus* (this study) and in macaque (other studies).

the point image size function proposed by Van Essen et al. ('84), was not found in the study by Dow et al. ('81) or in this study.

#### ACKNOWLEDGMENTS

The authors are grateful to Dr. E. Oswaldo-Cruz for helpful comments on the manuscript. Thanks are due to M. Fiorani, Jr., for help with the statistics, to Edil Saturato da Silva Filho for technical assistance, to Virginia P.G. Santos for the illustrations, and to Edna M. da Silva Ojeda for typing the manuscript. This research was supported by grants from CNPq (40.2829/84, 40.2577/85, 14.2440/85, 30.5654/76, 30.0188/80), FINEP (42.85.0245.00), and CEPG/UFRJ to the authors.

#### LITERATURE CITED

- Allman, J.M., and J.H. Kaas (1971) Representation of the visual field in striate and adjoining cortex of the owl monkey (*Aotus trivirgatus*). *Brain Res.* 35:89-106.
- Cowey, A. (1964) Projection of the retina onto striate and prestriate cortex in the squirrel monkey, *Saimiri sciureus*. *J. Neurophysiol.* 27:366-393.
- Daniel, P.M., and D. Whitteridge (1961) The representation of the visual field on the cerebral cortex in monkeys. *J. Physiol. London* 159:203-221.
- Dow, B.M., R.G. Snyder, R.G. Vautin, and R. Bauer (1981) Magnification factor and receptive field size in foveal striate cortex of the monkey. *Exp. Brain Res.* 44:213-228.
- Dow, B.M., R.G. Vautin, and R. Bauer (1985) The mapping of visual space onto foveal striate cortex in the macaque monkey. *J. Neurosci.* 5:890-902.
- Falk, D. (1980) Comparative study of the endocranial casts of New and Old World monkeys. In R.L. Ciochon and A.B. Chiarelli, (eds): *Evolutionary Biology of the New World Monkeys and Continental Drift*. New York: Plenum Press, pp. 275-292.
- Gallyas, F. (1979) Silver staining of myelin by means of physical development. *Neurol. Res.* 1:203-209.
- Gattass, R., and C.G. Gross (1981) Visual topography of the striate projection zone in the posterior superior temporal sulcus (MT) of the macaque. *J. Neurophysiol.* 46:621-638.
- Gattass, R., C.G. Gross, and J.H. Sandell (1981) Visual topography of V2 in the macaque. *J. Comp. Neurol.* 201:519-530.

- Gattass, R., A.P.B. Sousa, and E. Covey (1986) Cortical visual areas of the macaque: possible substrates for pattern recognition mechanisms. *Exp. Brain Res. (suppl) 11:1-20*.
- Gattass, R., A.P.B. Sousa, and M.G.P. Rosa (1984) Striate and extrastriate areas in the Cebus monkey: An electrophysiological and anatomical tracer study. *Proc. Soc. Neurosci. 10:474 (Abstract)*.
- Guld, C., and A. Bertulis (1976) Representation of fovea in the striate cortex of vervet monkey, *Cercopithecus aethiops pygerythrus*. *Vision Res. 16:629-631*.
- Hoffstetter, R. (1974) Phylogeny and Geographical Deployment of the Primates. *J. Hum. Evol. 3:327-350*.
- Le Vay, S., M. Connolly, J. Houde, and D.C. Van Essen (1985) The complete pattern of ocular dominance stripes in the striate cortex and visual field of the macaque monkey. *J. Neurosci. 5:486-501*.
- McIlwain, J.L. (1976) Large receptive fields and spatial transformations in the visual system. *Int. Rev. Physiol. 10:223-248*.
- Myerson, J., P.B. Manis, F.M. Miezin, and J.M. Allman (1977) Magnification in striate cortex and the retinal ganglion cell layer of the owl monkey: A quantitative comparison. *Science 198:855-857*.
- Piñon, M.C., A.P.B. Sousa, M.G.P. Rosa, and R. Gattass (1986) Aferentes corticais da área visual primária (V1) do macaco Cebus. *Proc. Soc. Brazilian Neurosci. 1:77*.
- Rosa, M.G.P., R. Gattass, and A.P.B. Sousa (1984) Split representation of the horizontal meridian in V2 in the Cebus monkey: A fluorescent tracer study. *Brazilian J. Med. Biol. Res. 17:410*.
- Sanides, F. (1972) Representation in the cerebral cortex and its areal lamination patterns. In G.H. Bourne (ed.): *The Structure and Function of Nervous Tissue*. New York: Academic Press, pp. 329-453.
- Shipp, S., and S.M. Zeki (1985) Segregation of pathways leading from area V2 to areas V4 and V5 of macaque monkey visual cortex. *Nature 315:322-325*.
- Talbot, S.A., and W.H. Marshall (1941) Physiological studies on neural mechanisms of visual localization and discrimination. *Am. J. Ophthalmol. 24:1255-1264*.
- Tootell, R.B.H., M.S. Silverman, E. Switkes, and R.L. De Valois (1982) Deoxyglucose analysis of retinotopic organization in primate striate cortex. *Science 218:902-904*.
- Van Essen, D.C., and J.H.R. Maunsell (1980) Two-dimensional maps of the cerebral cortex. *J. Comp. Neurol. 191:255-281*.
- Van Essen, D.C., W.T. Newsome, and J.H.R. Maunsell (1984) The visual field representation in striate cortex of the macaque monkey: Asymmetries, anisotropies and individual variability. *Vision Res. 24:429-448*.